Spinwave detection by nitrogen-vacancy centers in diamond as a function of probe–sample separation 🅕

C. M. Purser 🆔, V. P. Bhallamudi 🆔, F. Guo, M. R. Page 🆔, Q. Guo, G. D. Fuchs 🆔, and P. C. Hammel 🆔

COLLECTIONS

🅕 This paper was selected as Featured

View Online   Export Citation   CrossMark

Spinwave detection by nitrogen-vacancy centers in diamond as a function of probe–sample separation ⓕ

View Online   Export Citation   CrossMark

C. M. Purser,[1,a] ⓘ V. P. Bhallamudi,[2] ⓘ F. Guo,[3] M. R. Page,[1] ⓘ Q. Guo,[1,3] G. D. Fuchs,[3] ⓘ and P. C. Hammel[1] ⓘ

AFFILIATIONS

[1]Department of Physics, The Ohio State University, Columbus, Ohio 43210, USA
[2]Department of Physics, Indian Institute of Technology Madras, Chennai, TN 600036, India
[3]School of Applied and Engineering Physics, Cornell University, Ithaca, New York 14850, USA

[a]Author to whom correspondence should be addressed: purser.6@osu.edu

ABSTRACT

Magnetic field noise from magnons can reduce the lifetimes of proximate spins and degrade the performance of spin based technologies. However, spatial and temporal averaging over the area of typical field sensors makes measuring magnetic field noise challenging. Here, we use an ensemble of nitrogen-vacancy (NV) point-defects in diamond to measure the spectral profile of thermally excited spinwave noise at room temperature as a function of the distance away from a 20 nm thick Permalloy (Py) thin film. We systematically vary the separation between the NV and Py layers using a silicon-dioxide wedge and measure the longitudinal relaxation rate of the NV center $m_s = 0$ state as a function of the separation. The measured spinwave-induced relaxation of an ensemble of NV centers is well described by a magnetostatic model of dipole fields from the spinwaves. We furthermore find that our all-optical, nonperturbative measurements of the spinwave noise can be used to extract information about the ferromagnetic source, such as magnetization, damping, and fluctuating amplitude. This technique is amenable to application with stand-off from ferromagnetic elements and from buried structures.

Published under license by AIP Publishing. https://doi.org/10.1063/1.5141921

Thermal magnetic field noise can limit the performance of magnetic storage and logic technologies at the highest densities where individual bits are closely spaced. The spectrum and intensity of spin and charge noise from neighboring conducting, magnetic elements determine the design and placement of components.[1,2] An important capability for applications that require low magnetic field noise will be to measure the magnetic field noise intensity as a function of the distance away from each device component.

The negatively charged nitrogen-vacancy (NV) center in diamond has excellent sensitivity to fluctuating magnetic fields at room temperature and with high spatial resolution. The sensitivity can be further enhanced using an ensemble of spins by a scaling $\sqrt{N}$, where N is the number of NV spins. Because the NV center spin transition frequencies lie in the gigahertz regime, within the same band occupied by typical magnetic noise sources based on spinwaves, NV centers are well suited to studying thermal magnetic noise originating from the ferromagnetic material.[3–9]

Here, we measure the relaxation rate of NV centers in diamond proximate to thermally excited, incoherent spinwaves in a $Ni_{80}Fe_{20}$
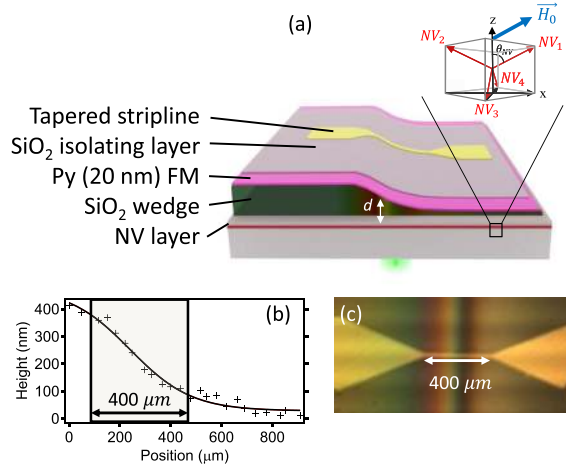
Permalloy (Py) thin film as a function of the separation from the film. A SiO_2 wedge separates a layer of implanted NV centers from the Py film, and by measuring the NV center spin lifetimes at different positions along the wedge, we are able to measure the noise of Py spinwaves as a function of NV-Py separation. We observe that the strength of fluctuating fields, as measured via monitoring the NV center spin relaxation rates, decreases monotonically with increasing separation, consistent with theoretical models.[4,7] Tuning the magnetic field strength controls the spectral overlap between NV center spin transition energies and the spectrum of ferromagnetic spinwaves, resulting in faster NV center spin relaxation rates when there is greater spectral overlap and NV center spin relaxation rates approaching the intrinsic kHz rates for minimal spectral overlap. We model the NV center spin relaxation rate as a function of the magnetic field and as a function of the NV-Py separation and find that the model agrees with the measured NV spin relaxation rates up to an overall scaling factor.

Combining the sensitivity of NV centers with thermal excitation of ferromagnetic spinwaves results in a measurement scheme that is noninvasive, in that the NV centers are passive sensors, and

nonperturbative, in that the ferromagnetic dynamics are not driven. We thus demonstrate a quantitative technique for measuring magnon dynamics in large M_s, metallic thin films relevant to information technology.

The separation between the NV and Py layers was controlled by a SiO_2 wedge patterned on the diamond surface as shown in Fig. 1(a). The NV centers were created by implanting an electronic-grade diamond with 50 ppm nitrogen ions ($^{14}N^+$) 50 nm below the diamond surface. The sample was subsequently annealed at 800 °C for 2 h and cleaned in an acid reflux bath of sulfuric acid and nitric acid for 3 h at 95 °C. To deposit the wedge, the diamond was placed beneath a shadow mask,[10] a 150 μm-thick glass cover slide fixed 300 μm above the diamond surface such that the edge of the mask was centered along one edge of the diamond chip. 500 nm of SiO_2 was RF sputtered at 300 W in a 1 mT Ar environment, resulting in a 0.2 Å/s deposition rate. The 20 nm Py film was deposited directly on the SiO_2 wedge. This Py layer was capped with Ti(5 nm)/SiO_2 (150 nm) to electrically isolate Py from the microwave (MW) strip line. The patterned microwave strip line tapers to a 20 μm × 400 μm constriction and 350 nm thick in total: Ti(5 nm)/Cu(335 nm)/Au(10 nm). The wedge profile [Fig. 1(b)] was obtained from AFM scans along a hard edge. The boxed region in (b) corresponds to the 400 μm-long constriction in the MW antenna, shown in an optical image of the sample [Fig. 1(c)]. The total NV-Py separation, d, is given by the wedge height at a particular point along the strip line plus the 50 ± 10 nm NV implantation depth.
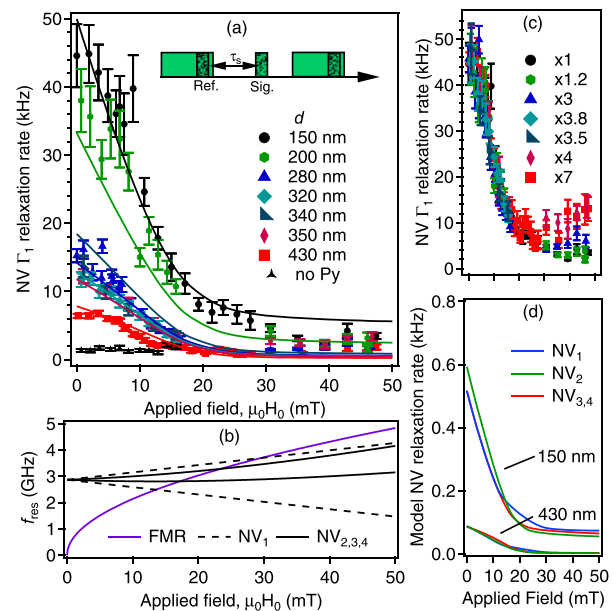
Field noise at the resonant frequency of the NV center spin transitions reduces its spin lifetime, which can be measured using a T_1 detection sequence. The NV center is initialized by illuminating the centers with 532 nm light that cyclically polarizes the spins into the $m_s = 0$ state. A reference gate ("Ref.") collects fluorescence at the end of the polarization pulse and serves as a reference that will normalize the fluorescence collected during a subsequent signal ("Sig.") gate.

Turning the laser off for time τ_s allows the NV center spin to interact with resonant fluctuating fields from phonons and proximate ferromagnetic magnons. These cause NV center spin transitions between the $m_s = 0$ and ± 1 spin states and hence relax the NV spin. The decay in fluorescence intensity, measured during a signal detection gate, measures the decay in the $m_s = 0$ spin state during τ_s. Because this protocol does not require resonant drive of the NV center spin transitions, the NV center spin transitions can be tuned through ferromagnetic resonance (FMR) without perturbing the underlying ferromagnetic dynamics. A timing diagram is presented as an inset to Fig. 2(a). Scanning τ_s reveals an exponentially decreasing normalized fluorescence N_{Sig}/N_{Ref}, where N is the number of photons counted during each gate. The decay constant Γ_1 measures the NV center spin relaxation rate.

In Fig. 2(a), the NV center spin relaxation rate Γ_1 is plotted as a function of the applied magnetic field for several NV-Py separations, d. The applied magnetic field is aligned to the NV_1 axis as shown in the inset to Fig. 1(a) and changes the magnetic resonance conditions of the NV centers and the ferromagnet, as shown in Fig. 2(b). The transition frequency of NV centers is governed by Zeeman splitting between the $+1$ and -1 spin states and by a zero-field splitting (2.87 GHz) between the $m_s = 0$ and $m_s = \pm 1$ spin states in the electronic ground state. For Py thin films with magnetization oriented in-plane, spinwaves occur at frequencies greater than the FMR frequency. Thus, at fields greater than 30 mT, when the NV resonances are lower than Py FMR, there is less spectral overlap with $k \neq 0$ spinwaves. Without noise at NV transition frequencies, the NV center spin

FIG. 1. Sample schematic. (a) A sputtered SiO_2 wedge separates a 20 nm film of Py and an implanted layer of NV centers 50 nm beneath the diamond surface. A tapered strip line is used to apply microwave fields in order to measure the magnetic field strength by monitoring the NV resonance line splitting. (b) Wedge profile with the boxed region corresponding to the stripline constriction. (c) Optical image of the sample with the 400 μm long constriction. The color variation appears due to thin-film interference in the SiO_2 layer.

FIG. 2. Spin lifetime measurements of the NV center in the presence of a ferromagnet. (a) Γ_1 as a function of the magnetic field for NV centers at different distances, d, from the Py film. Solid lines are the results of a fit by hand for M_s, α, Γ_0, and C. (b) Resonance dispersions for the ferromagnetic resonance (FMR) and NV transitions. (c) Scaling the data in (a) with respect to the NV spin relaxation rate at the lowest field. Colors and symbols correspond to those in (a). (d) Calculation results for NV spin relaxation rates as a function of the applied field for NV centers at different orientations [given in the inset of Fig. 1(a)] for $d = 150$ nm and 430 nm.

relaxation rates return to their intrinsic kilohertz values. Data collected for NV centers at 150 nm of SiO_2 and in the absence of Py are also presented in Fig. 2(a), demonstrating that the field-dependent spin relaxation rates are dominated by the effect of the ferromagnetic film.

As the separation, d, between the NV center layer and the Py layer increases, the dipole field strength from spinwaves decreases and the NV response weakens. This can be seen in Fig. 2(a) in which the relaxation rate for NV centers nearest the Py film is 45 kHz, while it is 6 kHz for NV centers farthest from the Py film. The monotonic decrease in coupling strength as a function of separation d is described by a filter function ke^{-2kd}, where the resonant spinwave has wavevector $\mathbf{k}$.[4,7] The k-dependence of this filter function becomes clear when one realizes that the $k = 0$ uniform mode does not produce stray magnetic fields, resulting in no NV spin relaxation. However, for spinwaves with $k \gg 1/d$, the dipole fields associated with the spinwaves average out and have negligible effects on the NV spin relaxation rate. The coupling strength is therefore nonmonotonic in k; however, the spinwave field strength decreases monotonically with separation, d, as observed for a given applied field in Fig. 2(a).

Figure 2(c) shows that the NV spin relaxation rates in Fig. 2(a) due to spinwaves in Py can be scaled with respect to one another and made to overlap at low fields (scaling factors are noted in the legend). Similar field dependences of the scaled data at different separations are due to the large magnetization in Py ($\sim$1 T). As the magnetization increases, a broader range of k-vectors are degenerate so that spinwave noise that relaxes the NV centers originates from a broad range of spinwave k-vectors. For ferromagnets with smaller magnetization, such as yttrium-iron garnet (YIG), only a narrow range of k-vectors match the spin resonance frequencies of the NV centers, such that a magnetic field dependence for one NV-ferromagnet separation is sufficient to determine the NV-ferromagnet separation. However, for the large M_s Py film used here, we find that it is necessary to simultaneously fit several separations in order to determine the best model parameters for the Py film.

NV center spins relax when coupled to dipole fields that fluctuate at frequencies resonant with NV center spin transitions and that have field projections transverse to the NV spin quantization axis. Here, we present a calculation of the strength and orientation of the time dependent dipole fields generated by spinwaves. The solid lines in Fig. 2(a) are the average of modeled NV spin relaxation rates for all NV center bond directions [shown for 150 nm and 430 nm in Fig. 2(d)], taken as representative of the measured NV relaxation rate due to the relative strength of the spinwave-induced relaxation over the intrinsic NV center spin relaxation [Fig. 2(a)] and due to the similarities in these calculated rates for a given d [Fig. 2(d)]. To find the best fit, model values are varied between 7×10^5 A/m and 9×10^5 A/m for M_s and between 0.005 and 0.02 for damping parameter α. The intrinsic NV spin relaxation rate Γ_0 and an overall scaling factor C are then modified to find the best fit to the data for all separations and magnetic fields simultaneously. We find that the data are best described by $M_s = 8 \times 10^5$ A/m, $\alpha = 0.015$, $\Gamma_0 = 0$, and $C = 81 \pm 10$. The magnetization and damping match well with literature values, though the damping is greater than the usual value of 0.01. The scaling factor C indicates that the model underestimates the measured field noise by a factor of 81, a discrepancy that may arise from our having neglected the effect of pinning sites and film inhomogeneities, and the assumption that each magnon contributes one Bohr magneton μ_B.[11]

An NV center in a single-crystal diamond will be oriented along one of four bond directions and, in general, have one of eight different $m_s = 0$ relaxation rates, two per bond orientation. In our sample geometry, we have three distinct NV spin relaxation rates, shown in Fig. 2(d) for $d = 150$ nm and 430 nm. Given the similarity in these rates for a given field strength and d, the NV fluorescence decay as a function of τ_s is fit with a single exponential time-constant, Γ_1, which we model as the average of the rates calculated for the four NV center bond orientations.

Following the formalisms presented in previous work,[4,7] the NV center spin relaxation rate for an NV center spin transition is

$$\Gamma_1(d) = \Gamma_0 + \sum_{\pm} \int \mathcal{D}(\omega_{\pm}, \boldsymbol{k})\mathcal{F}(\boldsymbol{k}, d)d\boldsymbol{k}, \qquad (1)$$

where $\omega_{\pm}$ is the frequency of an NV center spin resonance. $\mathcal{D}(\omega_{\pm}, \boldsymbol{k})$ is the spectral overlap between spinwave $\boldsymbol{k}$ and $\omega_{\pm}$, $\mathcal{F}(\boldsymbol{k}, d)$ is the dipole coupling strength between thermally excited spinwaves and NV-center spins, and Γ_0 is the intrinsic NV spin relaxation rate.

Frequency matching $\mathcal{D}(\omega_{\pm}, \boldsymbol{k})$ is determined by the spectral overlap between NV transition frequencies ($\omega_{\pm}$) and spinwave dispersions $\omega_k(\mathbf{k})$.[12] The overlap is given by a Lorentzian function with maximum at $\omega_k = \omega_{\pm}$ and is given by $\frac{1}{\pi}\frac{\alpha\omega_k}{(\alpha\omega_k)^2 + (\omega_{\pm} - \omega_k)^2}$. We find that the data are best fit with a spinwave damping of $\alpha = 0.015$.

The stray magnetic field strength and orientation from spinwaves are calculated using a magnetostatic model that treats spinwaves as fluctuating distributions of effective magnetic charge densities,[13] $\rho = \nabla \cdot \mathbf{m_k}$, where $\mathbf{m_k}$ is the fluctuating component of the magnetization, assumed here to be in-plane and transverse to the equilibrium magnetization. Thus, for spinwaves propagating parallel to the equilibrium magnetization direction, $\rho \sim 0$, and the stray dipole-field strength is effectively zero. For spinwaves propagating perpendicular to the equilibrium magnetization direction, $\rho \neq 0$, and the stray dipole-field strength is nonzero. The spatial variation of spinwave moments is given by

$$\mathbf{M}(\mathbf{r}) = \mathbf{M}_0 + \sum_k \mathbf{m}_k(z) e^{i\mathbf{k}\cdot\mathbf{r}} \quad -t/2 \leq z \leq t/2, \qquad (2a)$$

$$\mathbf{M}(\mathbf{r}) = 0 \quad |z| > t/2, \qquad (2b)$$

where t is the film thickness centered about $z = 0$. The solution for the magnetostatic potential, $\Phi_k(z)$, determines $\mathbf{h_k} = -\nabla\Phi_k(z)$, the dipole fields above the ferromagnetic film. Spin relaxation is sensitive to squared projections of these dipole fields onto planes transverse to NV center spin quantization axes (quantization axes are assumed to be the NV center bond axis for the low fields used in this work). For NV_1 and NV_2, as defined in Fig. 1,

$$\mathcal{F}(\boldsymbol{k}, d) = \gamma^2 \mu_0^2 m_y^2 \left\{ \frac{\sin^2(2\phi_k)}{4} \cos^2(\theta_{NV}) + \sin^4(\phi_k) \right.$$
$$\left. + \sin^2(\phi_k) \sin^2(\theta_{NV}) \right\} \left\{ \frac{1}{4} e^{-2kd}(1 - e^{-kt})^2 \right\}. \qquad (3)$$

For NV_3 and NV_4,

$$\mathcal{F}(\boldsymbol{k}, d) = \gamma^2 \mu_0^2 m_y^2 \left\{ \frac{\sin^2(2\phi_k)}{4} + \sin^4(\phi_k) \cos^2(\theta_{NV}) \right.$$
$$\left. + \sin^2(\phi_k) \sin^2(\theta_{NV}) \right\} \left\{ \frac{1}{4} e^{-2kd}(1 - e^{-kt})^2 \right\}. \qquad (4)$$
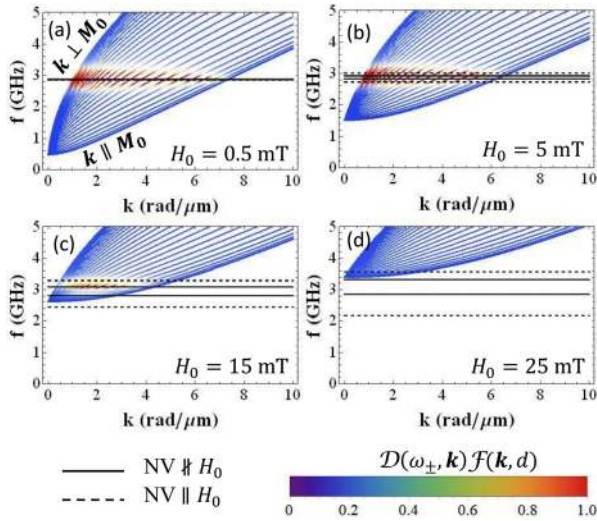
FIG. 3. Coupling parameter $\mathcal{D}(\mathbf{k}, \omega_{\pm})\mathcal{F}(\mathbf{k}, d)$ between different NV resonances (black horizontal lines) and an individual spinwave for different values of k and ϕ_k for (a) 0.5 mT, (b) 5 mT, (c) 15 mT, and (d) 25 mT. Increasing field strength moves the spinwave manifold upward in frequency [where $k = 0$ matches the resonance condition shown in Fig. 2(b)].

The relationship between the number of spinwaves, $N_{\omega,k}$, and the transverse magnetization can be estimated from the following expression for the change in the Py longitudinal magnetization, M_x, from the ground-state magnetization $M_0 = M_s$:

$$M_x^2 = M_0^2 - (m_y^2 + m_z^2), \tag{5a}$$

$$M_x = M_0 - \frac{m_y^2}{2M_0}, \tag{5b}$$

where we assume that $m_y \ll M_0$ and m_z, the out-of-plane component of fluctuating magnetization, is approximately zero. Since each spinwave reduces the total magnetization by one quantum, $N_{\omega,k}$ spinwaves will reduce the magnetization by $\frac{N_{\omega,k}}{V} g_L \mu_B$, for Landé g-factor $g_L = 2$. Thus, the change in magnetization is

$$M_x = M_0 - \frac{N_{\omega,k}}{V} g_L \mu_B. \tag{6}$$

We can then make the approximation that $m_y^2 = 2M_s \frac{N_{\omega,k}}{V} g_L \mu_B$.

The number of thermally excited spinwaves $N_{\omega,k}$ is estimated by assuming occupancy according to the Rayleigh–Jeans distribution,[7] $\frac{k_B T}{\hbar \omega}$, and the 2D density of states in k-space ($A/4\pi^2$, for sample area A) for spinwaves with in-plane wavevectors. Finally, the quantity m_y^2 can be expressed quantitatively in terms of sample properties as

$$m_y^2 = \frac{2M_s g_L \mu_B}{V} \frac{A}{4\pi^2} \frac{k_B T}{\hbar \omega_k}, \tag{7}$$

where the factor A/V is given by $1/t$, for film thickness $t = 20$ nm.

The combined integrand $\mathcal{D}(\omega_{\pm}, \mathbf{k})\mathcal{F}(\mathbf{k}, d)$ for all four NV center bond orientations and spin transitions is presented in Fig. 3 in k-space. As expected, the strength of the coupling is the strongest where

the NV center spin resonances overlap with spinwaves. Due to the ϕ_k dependence of dipole fields from spinwaves, the coupling is zero for $\mathbf{k} \parallel \mathbf{M}_0$ or $\phi_k = 0$.

We demonstrate that NV centers provide room-temperature sensitivity to thermally excited field fluctuations from ferromagnetic structures. This sensitivity points to several applications including sensing field noise from device components, measuring spinwave excitations that cannot be directly probed using inductive techniques (such as symmetric localized modes in confined structures) and measuring ferromagnetic properties in hybrid systems where ferromagnets may be screened from microwave drive fields.

The noninvasive, nonperturbative approach demonstrated in this work provides an attractive method for sensing spinwaves, which enables a measure of M_s, linewidth, and strength of fluctuating magnetization. Determining these parameters from the NV spin relaxation rates requires a separation dependence for large M_s ferromagnets, which can be implemented with recently developed NV-based scan probes. By increasing the precision of measured NV center spin relaxation rates or by probing noise with one NV orientation, a similar experiment could potentially measure the ellipticity of spinwave precession, an important quantity for spin-transport based devices.[14]

REFERENCES

[1] N. Stutzke, S. L. Burkett, and S. E. Russek, Appl. Phys. Lett. **82**, 91 (2003).

[2] N. Smith, J. Appl. Phys. **90**, 5768 (2001).

[3] C. S. Wolfe, V. P. Bhallamudi, H. L. Wang, C. H. Du, S. Manuilov, R. M. Teeling-Smith, A. J. Berger, R. Adur, F. Y. Yang, and P. C. Hammel, Phys. Rev. B **89**, 180406 (2014).

[4] T. van der Sar, F. Casola, R. Walsworth, and A. Yacoby, Nat. Commun. **6**, 8426 (2015).

[5] C. S. Wolfe, S. A. Manuilov, C. M. Purser, R. Teeling-Smith, C. Dubs, P. C. Hammel, and V. P. Bhallamudi, Appl. Phys. Lett. **108**, 232409 (2016).

[6] M. R. Page, B. A. McCullian, C. M. Purser, J. G. Schulze, T. M. Nakatani, C. S. Wolfe, J. R. Childress, M. E. McConney, B. M. Howe, P. C. Hammel, and V. P. Bhallamudi, J. Appl. Phys. **126**(12), 124902 (2019).

[7] C. Du, T. van der Sar, T. X. Zhou, P. Upadhyaya, F. Casola, H. Zhang, M. C. Onbasli, C. A. Ross, R. L. Walsworth, Y. Tserkovnyak, and A. Yacoby, Science **357**, 195 (2017).

[8] P. Andrich, C. F. de las Casas, X. Liu, H. L. Bretscher, J. R. Berman, F. J. Heremans, P. F. Nealey, and D. D. Awschalom, NPJ Quantum Inf. **3**, 28 (2017).

[9] D. Kikuchi, D. Prananto, K. Hayashi, A. Laraoui, N. Mizuochi, M. Hatano, E. Saitoh, Y. Kim, C. A. Meriles, and T. An, Appl. Phys. Express **10**, 103004 (2017).

[10] S. Kolkowitz, A. Safira, A. A. High, R. C. Devlin, S. Choi, Q. P. Unterreithmeier, D. Patterson, A. S. Zibrov, V. E. Manucharyan, H. Park, and M. D. Lukin, Science **347**, 1129 (2015).

[11] A. Gurevich and G. Melkov, *Magnetization Oscillations and Waves* (Taylor & Francis, 1996).

[12] B. A. Kalinikos and A. N. Slavin, J. Phys. C **19**, 7013 (1986).

[13] K. J. Harte, J. Appl. Phys. **39**, 1503 (1968).

[14] S. Singh, J. Katoch, T. Zhu, K.-Y. Meng, T. Liu, J. T. Brangham, F. Yang, M. E. Flatté, and R. K. Kawakami, Phys. Rev. Lett. **118**, 187201 (2017).